

SLIDING MODE POSITION CONTROL FOR REAL-TIME CONTROL OF INDUCTION MOTORS

OSCAR BARAMBONES¹, PATXI ALKORTA² AND JOSE MARIA GONZALEZ DE DURANA¹

¹Engineering School of Vitoria
University of the Basque Country
Nieves Cano 12, 01012 Vitoria, Spain
oscar.barambones@ehu.es

²Engineering School of Eibar
University of the Basque Country
Otaola 29. 20600 Eibar, Spain
patxi.alkorta@ehu.es

Received April 2012; revised August 2012

ABSTRACT. *A sliding mode position control for high-performance real-time applications of induction motors is developed in this work. The design also incorporates a simple flux estimator in order to avoid the flux sensors. Then, the proposed control scheme presents a low computational cost and therefore can be implemented easily in a real-time applications using a low cost DSP-processor. The stability analysis of the controller under parameter uncertainties and load disturbances is provided using the Lyapunov stability theory. Finally, simulated and experimental results show that the proposed controller with the proposed observer provides a good trajectory tracking and that this scheme is robust with respect to plant parameter variations and external load disturbances.*

Keywords: Position control, Sliding mode control, Robust control, Induction machines, Lyapunov stability, Nonlinear control

1. Introduction. AC induction motors have been widely used in industrial applications such as machine tools, steel mills and paper machines owing to their good performance provided by their solid architecture, low moment of inertia, low ripple of torque and high initiated torque. Some control techniques have been developed to regulate these induction motor servo drives in high-performance applications. One of the most popular technique is the indirect field oriented control method [1, 2].

The field-oriented technique guarantees the decoupling of torque and flux control commands of the induction motor, so that the induction motor can be controlled linearly as if it were a separated excited D.C. motor. However, the control performance of the resulting linear system is still influenced by uncertainties, which usually are composed of unpredictable parameter variations, external load disturbances, and unmodelled and nonlinear dynamics.

In the last decades the proportional integral derivative (PID) controller has been widely used in the vector control of induction motors due to its good performance and its simple structure. However, in some applications the PID controller may not meet the concerned robustness under parameter variations and external load disturbances. Therefore, many studies have been made on the motor drives in order to preserve the performance under these parameter variations and external load disturbances, such as nonlinear control [3, 4], adaptive control [5], robust control, fuzzy control and neural control. However, usually these controllers present a high computational cost and cannot be implemented over a low cost DSP processor to perform a real time control.

The sliding-mode control can offer many good properties, such as good performance against unmodelled dynamics, insensitivity to parameter variations, external disturbance rejection and fast dynamic response. These advantages of the sliding-mode control may be employed in the position and speed control of an AC servo system [6]. In [7] an integral sliding mode position control for induction motor based on field oriented control theory is proposed. In the work of [8], an integrated sliding mode controller (SMC) based on space vector pulse width modulation method is proposed to achieve high-performance speed control of an induction motor. In this work using a field-oriented control principle, a flux SMC is first established to achieve fast direct flux control and then a speed SMC is presented to enhance speed control by the direct torque method. However, in this work the performance of the proposed controller is not validated over a real induction motor. In recent literatures, the integral sliding mode control (ISMC) method is introduced in the control design of speed loop in order to improve the disturbance rejection property of speed control system for a permanent magnet synchronous motor.

Position control is often used in some applications of electrical drives like robotic systems, conveyor belts. In these applications uncertainty and external disturbances are present and therefore a robust control system that maintains the desired control performance under this situations is frequently required [9, 10]. In the work of [11] the neural networks are employed to approximate the nonlinearities and an adaptive backstepping technique is used to construct the controller for the position tracking control of induction motors with parameter uncertainties and load torque disturbance. The H_∞ control design problem for a high performance hard disk drive servo controller is solved by Genetic Algorithm in the work of [12]. The proposed technique does not only solve the problem of high order controller in the conventional design, but also still retains the robust performance of conventional H_∞ control technique. The variable structure control strategy using the sliding-mode has also been focused on many studies and research for the position control of the induction motors [13, 14].

The induction motor position control problem has been recently studied in [15] using a discrete time sliding mode control. The field oriented control theory is also used in order to decouple the flux and the electromagnetic torque. In this paper the authors calculate the rotor flux vector angular position using the slip estimates which is very sensitive to the rotor resistance variation.

On the other hand, in the last decade remarkable efforts have been made to reduce the number of sensors in the control systems [16, 17]. The sensors increase the cost and also reduce the reliability of the control system because these elements are generally expensive, delicate and difficult to instal.

In this paper, a robust approach for induction motor position control is presented. The proposed sliding mode control may overcome the system uncertainties and load disturbances that usually are present in the real systems. In the controller design, the field oriented control theory is used to simplify the system dynamical equations. Moreover, the proposed controller does not present a high computational cost and therefore can be implemented easily in a real-time applications using a low cost DSP-processor.

In this work, a flux estimation algorithm, based on a Luenberger observer, is also proposed in order to avoid the flux sensors. This observer presents a low computational cost and therefore is adequate as well to be implemented in real time applications using a low cost DSP-processor. The proposed observer uses a state space plant model and incorporates a feedback loop using the difference between the measured stator currents and the state space model stator currents in order to overcome the system model uncertainties. The estimated rotor flux is used to calculate the rotor flux vector angular position whose value is essential in order to apply the field oriented control principle.

Moreover, the control scheme presented in this paper is validated in a real test using a commercial induction motor of 7.5 kW in order to demonstrate the real performance of this controller. The experimental validation has been implemented using a control platform based on a DS1103 PPC Controller Board that has been designed and constructed in order to carry out the experimental validation of the proposed controller.

This manuscript is organized as follows. The flux observer is introduced in Section 2. Then, the proposed variable structure robust position control is presented in Section 3. In Section 4, the experimental control platform is presented and some simulation and experimental results are carried out. Finally, concluding remarks are stated in Section 5.

2. Rotor Flux Estimator. Many schemes based on simplified motor models have been devised to estimate some internal variables of the induction motor from measured terminal quantities [22]. This procedure is frequently used in order to avoid the presence of some sensors in the control scheme. In order to obtain an accurate dynamic representation of the motor, it is necessary to base the calculation on the coupled circuit equations of the motor.

Since the motor voltages and currents are measured in a stationary frame of reference, it is also convenient to express the induction motor dynamical equations in this stationary frame.

The system state space equations in the stationary reference frame can be written in the form [22]:

$$\dot{x} = Ax + Bv_s \quad (1)$$

where

$$x = [i_{ds} \quad i_{qs} \quad \psi_{dr} \quad \psi_{qr}]^T$$

$$v_s = [v_{ds} \quad v_{qs}]^T$$

$$B = \begin{bmatrix} \frac{1}{\sigma L_s} & 0 & 0 & 0 \\ 0 & \frac{1}{\sigma L_s} & 0 & 0 \end{bmatrix}^T$$

$$A = \begin{bmatrix} -\rho & 0 & \frac{R_r}{c L_r} & \frac{w_r}{c} \\ 0 & -\rho & -\frac{w_r}{c} & \frac{R_r}{c L_r} \\ \frac{L_m R_r}{L_r} & 0 & -\frac{R_r}{L_r} & -w_r \\ 0 & \frac{L_m R_r}{L_r} & w_r & -\frac{R_r}{L_r} \end{bmatrix}$$

where $\rho = \frac{L_m^2 R_r + L_r^2 R_s}{\sigma L_s L_r^2}$ and $c = \frac{\sigma L_s L_r}{L_m}$.

Considering the stator currents as the system output, the output equation for this system is:

$$y = Cx \quad (2)$$

where

$$C = \begin{bmatrix} 1 & 0 & 0 & 0 \\ 0 & 1 & 0 & 0 \end{bmatrix}$$

Then, the states observer, which estimates the system states (stator current and rotor flux), is defined by means of the following equation (Luenberger observer):

$$\dot{\hat{x}} = A\hat{x} + Bv_s + G(y - C\hat{x}) \quad (3)$$

$$= A\hat{x} + Bv_s + GC(x - \hat{x}) \quad (4)$$

where the symbol $(\hat{\cdot})$ represents the estimated values and G is the observer gain matrix.

Therefore, if the observer gain G is chosen such that the characteristic equation of the matrix $A - GC$ has all its roots with a negative real part, then the estimation error converges to zero. Consequently the estimated states \hat{i}_{ds} , \hat{i}_{qs} , $\hat{\psi}_{ds}$, $\hat{\psi}_{qs}$ converges to the real states i_{ds} , i_{qs} , ψ_{ds} , ψ_{qs} as t tends to infinity. Hence, the rotor flux may be obtained from the state observer given by Equation (3).

3. Variable Structure Robust Position Control. The mechanical equation of an induction motor can be written as:

$$J\ddot{\theta}_m + B\dot{\theta}_m + T_L = T_e \quad (5)$$

where J and B are the inertia constant and the viscous friction coefficient of the induction motor respectively; T_L is the external load; θ_m is the rotor mechanical position, which is related to the rotor electrical position, θ_r , by $\theta_m = 2\theta_r/p$ where p is the pole numbers and T_e denotes the generated torque of an induction motor, defined as [22]:

$$T_e = \frac{3pL_m}{4L_r}(\psi_{dr}^e i_{qs}^e - \psi_{qr}^e i_{ds}^e) \quad (6)$$

where ψ_{dr}^e and ψ_{qr}^e are the rotor-flux linkages, with the subscript 'e' denoting that the quantity is referred to the synchronously rotating reference frame; i_{qs}^e and i_{ds}^e are the stator currents, and p is the pole numbers.

The estimated angular position of the rotor flux vector ($\bar{\psi}_r$) related to the d -axis of the stationary reference frame may be calculated by means of the rotor flux components in this reference frame ($\hat{\psi}_{dr}$, $\hat{\psi}_{qr}$) as follows:

$$\hat{\theta}_e = \arctan\left(\frac{\hat{\psi}_{qr}}{\hat{\psi}_{dr}}\right) \quad (7)$$

where $\hat{\theta}_e$ is the estimated angular position of the rotor flux vector.

Using the field-orientation control principle, the current component i_{ds}^e is aligned in the direction of the rotor flux vector $\bar{\psi}_r$, and the current component i_{qs}^e is aligned in the perpendicular direction to it. At this condition, it is satisfied that:

$$\psi_{qr}^e = 0, \quad \psi_{dr}^e = |\bar{\psi}_r| \quad (8)$$

Taking into account the results presented in Equation (8), the equation of induction motor torque (6) is simplified to:

$$T_e = \frac{3pL_m}{4L_r}\psi_{dr}^e i_{qs}^e = K_T i_{qs}^e \quad (9)$$

where K_T is the torque constant, defined as follows:

$$K_T = \frac{3pL_m}{4L_r}\psi_{dr}^{e*} \quad (10)$$

where ψ_{dr}^{e*} denotes the command rotor flux.

With the above mentioned proper field orientation, the dynamics of the rotor flux is given by:

$$\frac{d\psi_{dr}^e}{dt} + \frac{\psi_{dr}^e}{T_r} = \frac{L_m}{T_r} i_{ds}^e \quad (11)$$

Then, the mechanical Equation (5) becomes:

$$\ddot{\theta}_m + a\dot{\theta}_m + f = bi_{qs}^e \quad (12)$$

where the parameters are defined as:

$$a = \frac{B}{J}, \quad b = \frac{K_T}{J}, \quad f = \frac{T_L}{J} \quad (13)$$

Now, the previous mechanical Equation (12) is considered with uncertainties as follows:

$$\ddot{\theta}_m = -(a + \Delta a)\dot{\theta}_m - (f + \Delta f) + (b + \Delta b)i_{qs}^e \quad (14)$$

where the terms Δa , Δb and Δf represent the uncertainties of the terms a , b and f respectively.

Let us define the position tracking error as follows:

$$e(t) = \theta_m(t) - \theta_m^*(t) \quad (15)$$

where θ_m^* is the rotor position command.

Taking the second derivative of the previous equation with respect to time yields:

$$\ddot{e}(t) = \ddot{\theta}_m - \ddot{\theta}_m^* = u(t) + d(t) \quad (16)$$

where the following terms have been collected in the signal $u(t)$,

$$u(t) = bi_{qs}^e(t) - a\dot{\theta}_m(t) - f(t) - \ddot{\theta}_m^*(t) \quad (17)$$

and the uncertainty terms have been collected in the signal $d(t)$,

$$d(t) = -\Delta a\dot{\theta}_m(t) - \Delta f(t) + \Delta b i_{qs}^e(t) \quad (18)$$

Now, the sliding variable $S(t)$ is defined as:

$$S(t) = \dot{e}(t) + ke(t) + k_i \int e(t)dt \quad (19)$$

where k and k_i are a positive constant gains.

Then, the sliding surface is defined as:

$$S(t) = \dot{e}(t) + ke(t) + k_i \int e(t)dt = 0 \quad (20)$$

The sliding mode controller is designed as:

$$u(t) = -k\dot{e} - k_i e - \beta \operatorname{sgn}(S) \quad (21)$$

where k and k_i are the previously defined positive constant gains, β is the switching gain, S is the sliding variable defined in Equation (19) and $\operatorname{sgn}(\cdot)$ is the sign function.

Assumption. In order to obtain the position trajectory tracking, the gain β must be chosen so that $\beta \geq \bar{d}$ where $\bar{d} \geq \sup_{t \in R^{0+}} |d(t)|$. Note that this condition only implies that the system uncertainties are bounded magnitudes.

Theorem 3.1. Consider the induction motor given by Equation (14), the control law (21) leads the rotor mechanical position $\theta_m(t)$ so that the position tracking error $e(t) = \theta_m(t) - \theta_m^*(t)$ tends to zero as the time tends to infinity.

Proof: Define the Lyapunov function candidate:

$$V(t) = \frac{1}{2}S(t)S(t) \quad (22)$$

Its time derivative is calculated as:

$$\begin{aligned} \dot{V}(t) &= S(t)\dot{S}(t) \\ &= S \cdot [\ddot{e} + k\dot{e} + k_i e] \\ &= S \cdot [u + d + k\dot{e} + k_i e] \\ &= S \cdot [-k\dot{e} - k_i e - \beta \operatorname{sgn}(S) + d + k\dot{e} + k_i e] \\ &= S \cdot [d - \beta \operatorname{sgn}(S)] \\ &\leq -(\beta - |d|)|S| \\ &\leq 0 \end{aligned} \quad (23)$$

It should be noted that Equations (19), (16) and (21) have been used in the proof.

Using the Lyapunov's direct method, since $V(t)$ is clearly positive-definite, $\dot{V}(t)$ is negative definite and $V(t)$ tends to infinity as $S(t)$ tends to infinity, then the equilibrium at the origin $S(t) = 0$ is globally asymptotically stable. Therefore, $S(t)$ tends to zero as the time t tends to infinity. Moreover, all trajectories starting off the sliding surface $S = 0$ must reach it in finite time and then they will remain on this surface. This system's behavior, once on the sliding surface is usually called *sliding mode*.

When the sliding mode occurs on the sliding surface (20), then $S(t) = \dot{S}(t) = 0$, and therefore the dynamic behavior of the tracking problem (16) is equivalently governed by the following equation:

$$\dot{S}(t) = 0 \quad \Rightarrow \quad \ddot{e}(t) + k\dot{e}(t) + k_i e(t) = 0 \quad (24)$$

Then, like k and k_i are a positive constants, the tracking error $e(t)$ and its derivatives $\dot{e}(t)$ and $\ddot{e}(t)$ converges to zero exponentially.

It should be noted that, a typical motion under sliding mode control consists of a *reaching phase* during which trajectories starting off the sliding surface $S = 0$ move toward it and reach it in finite time, followed by *sliding phase* during which the motion will be confined to this surface and the system tracking error will be represented by the reduced-order model (24), where the tracking error tends to zero.

Finally, the torque current command, $i_{qs}^{e*}(t)$, can be obtained directly substituting Equation (21) in Equation (17):

$$i_{qs}^{e*}(t) = \frac{1}{b} \left[-k\dot{e} - k_i e - \beta \operatorname{sgn}(S) + a\dot{\theta}_m + \ddot{\theta}_m^* + f(t) \right] \quad (25)$$

It should be noted that the current command is a bounded signal because all its components are bounded.

Therefore, the proposed variable structure position control resolves the position tracking problem for the induction motor in presence of some uncertainties in mechanical parameters and load torque.

It should be pointed out that, as it is well known, the variable structure control signals may produce the so-called chattering phenomenon, caused by the discontinuity that appear in Equation (25) across the sliding surface. Chattering is undesirable in practice, since it involves high control activity and further may excite high-frequency dynamics. Fortunately, in the induction motor system, this high frequency changes in the electromagnetic torque will be filtered by the mechanical system inertia. Nevertheless, in order to reduce the chattering effect, the control law can also be smoothed out. In this case

a simple and easy solution (proposed in [23]) could be to replace the sign function by a tansigmoid function in order to avoid the discontinuity in the control signal.

4. Simulation and Experimental Results. In this section the position regulation performance of the proposed sliding-mode field oriented control versus reference and load torque variations is analyzed by means of different simulation examples and real test using a commercial induction motor.

The block diagram of the proposed robust position control scheme is presented in Figure 1, and the function of the blocks that appear in this figure are explained below:

The block ‘VSC Controller’ represents the proposed sliding-mode controller, and it is implemented by Equations (19) and (25). The block ‘limiter’ limits the current applied to the motor windings so that it remains within the limit value, being implemented by a saturation function. The block ‘ $dq^e \rightarrow abc$ ’ makes the conversion between the synchronously rotating and stationary reference frames (Park’s Transformation). The block ‘Current Controller’ consists of an SVPWM current control. The block ‘SVPWM Inverter’ is a six IGBT-diode bridge inverter with 540 V DC voltage source. The block ‘Field Weakening’ gives the flux command based on rotor speed, so that the PWM controller does not saturate. The block ‘ i_{ds}^{e*} Calculation’ provides the current reference i_{ds}^{e*} from the rotor flux reference through Equation (11). The block ‘Flux Estimator’ represents the proposed Flux estimator, and it is implemented by Equation (3). The block ‘ $\hat{\theta}_e$ Calculation’ provides the angular position of the rotor flux vector. Finally, the block ‘IM’ represents the induction motor.

In order to carry out the real experimental validation of the proposed control scheme, the control platform shown in Figure 2 is used. The block diagram of this experimental platform is shown in Figure 3.

This control platform allows to verify the real time performance of the induction motor controls in a real induction motor. The platform is formed by a PC with Windows XP in which it is installed MatLab7/Simulink R14 and ControlDesk 2.7 and the DS1103 Controller Board real time interface of dSpace. The power block is formed of a three-phase rectifier connected to 380 V/50 Hz AC electrical net and a capacitor bank of 27.200 μ F in order to get a DC bus of 540 V. The platform also includes a three-phase IGBT/Diode

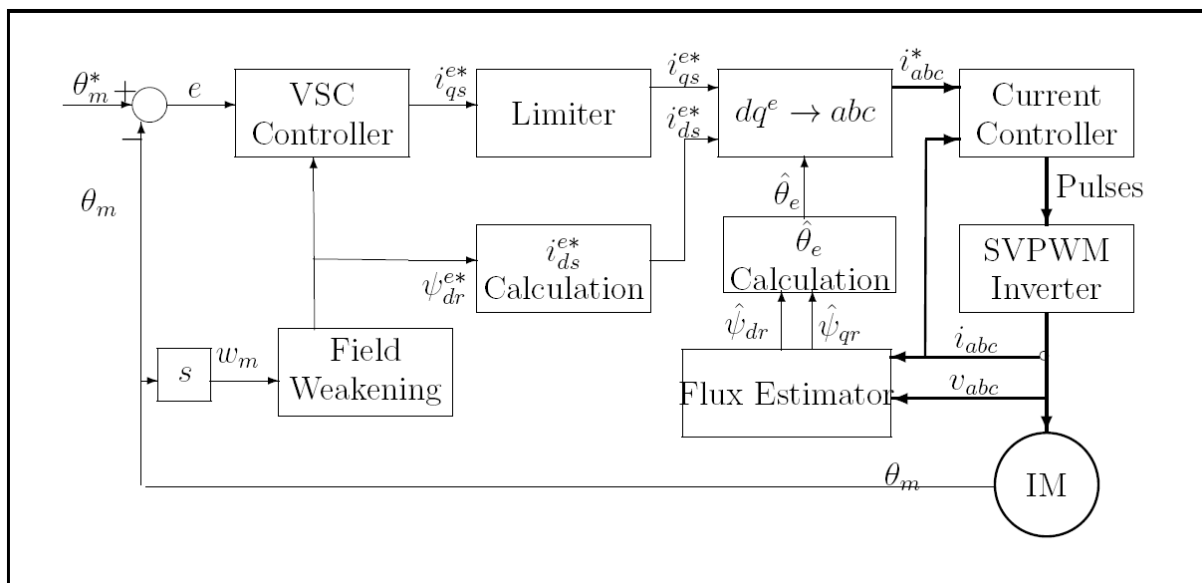


FIGURE 1. Block diagram of the proposed sliding-mode field oriented control

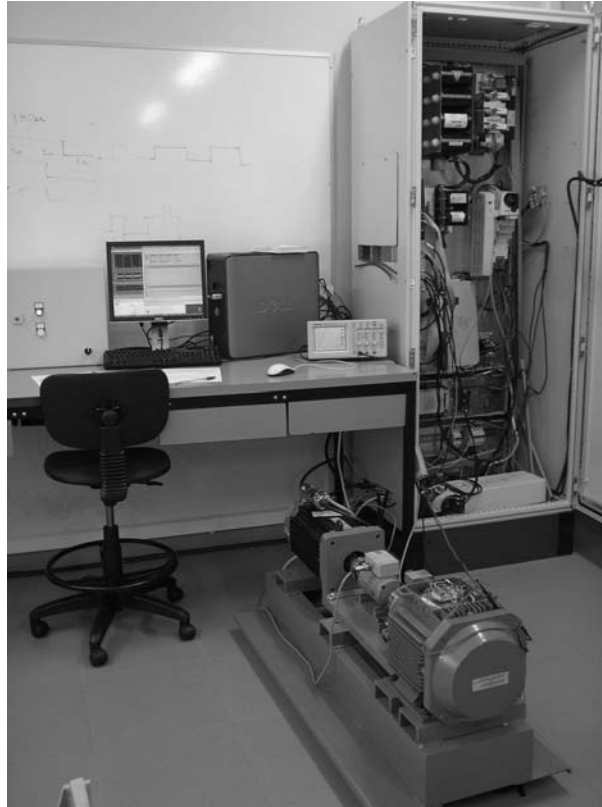


FIGURE 2. Induction motor experimental platform

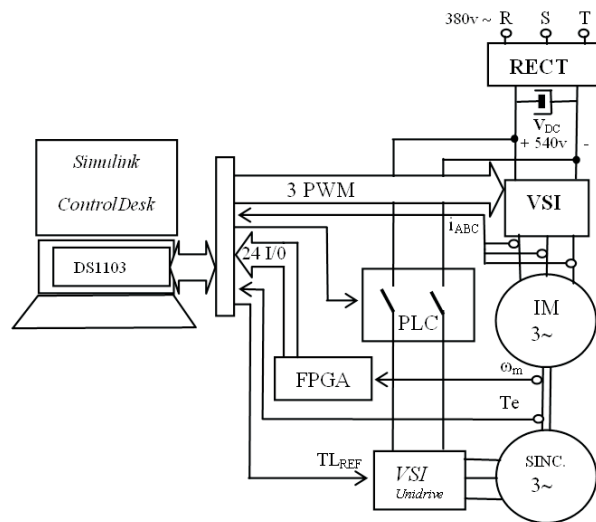


FIGURE 3. Block diagram of the induction motor experimental platform

bridge of 50 A, and the M2AA 132M4 ABB induction motor of 7.5 kW of die-cast aluminium squirrel-cage type and 1440 rpm, with the following parameters given by the manufacturer:

- R_s , stator resistance, 0.81Ω
- R_r , rotor resistance, 0.57Ω
- L_m , magnetizing inductance, 0.117774 mH
- L_s , stator inductance, 0.120416 mH
- L_r , rotor inductance, 0.121498 mH

- p , pair of poles, 2
- J , moment of inertia, 0.057 kg m^2
- B , viscous friction coefficient, $0.015 \text{ N m/(rad/s)}$
- α_{Al} , temperature coefficient of Aluminium, 0.0039 K^{-1}

The rotor position of this motor is measured using the G1BWGLDBI LTN incremental rotary encoder of 4096 square impulses per revolution. This pulses are quadruplicated in a decoder, giving a resolution of 16384 ppr which gives an angle resolution of 0.000385 rad (0.022 deg).

The platform also includes a 190U2 Unimotor synchronous AC servo motor of 10.6 kW connected to the induction motor to generate the load torque (controlled in torque). This servo motor is controlled by its VSI Unidrive inverter module.

The sample time used to realize the real implementation of the position control is $100 \mu\text{s}$, and the processor used for the real tests is a floating point PowerPC at 1 MHz, located in the real time DS1103 hardware of dSpace. This target incorporates the TMS320F240 DSP working as slave to generate the SVPWM pulses for the inverter. Finally, the position and currents control algorithms, the θ_e angle and flux estimator, the SVPWM calculations, and the Park's transformations have been realized in C programming language in a unique S-Builder module of Simulink, in order to obtain a compact and portable code.

In the experimental validation it is assumed that there is an uncertainty around 50% in the system mechanical parameters, which will be overcome by the proposed variable structure control. The rotor flux of the induction motor has been set to its nominal value of 1.01 Wb, keeping the flux current command, i_{sd}^* , to a constant value of 8.61 A. On the other hand, the electromagnetic torque current command, i_{sq}^* , has been limited to 20 A, in order to provide a protection against overcurrents in the induction motor's stator fed. Finally, the frequency of commutation of VSI module of the platform is limited to 8 kHz.

In this example a square wave position reference (similar to the reference proposed in [15]) is chosen. The square wave position reference is a good reference for a testing purposes and is widely used; however, a real system can not track this reference with a zero error in the steps, because the reference value changes in a zero time period.

In the experimental validation the motor starts from a standstill state and it is required that the rotor position follows a square wave position command, whose amplitude varies between 0 and 15 rad and whose frequency is 0.125 Hz. The system starts with an initial load torque $T_L = 0 \text{ N.m}$, and at time $t = 1 \text{ s}$, the load torque steps from $T_L = 0 \text{ N.m}$ to $T_L = 20 \text{ N.m}$, which is a 50% of the nominal torque value.

In this example the following values have been chosen for the controller parameters, $k = 44$, $k_i = 460$ and $\beta = 200$.

Finally, in order to reduce the chattering, the current command is passed through a low pass filter of 200 rad/s.

Figure 4 shows the simulation test of the proposed variable structure position control for the induction motor. The first graph shows the reference and the real rotor position. As it can be seen, the rotor position tracks the reference position in spite of system uncertainties. Obviously, when the reference steps from the 0 to 15 rad instantaneously, the rotor position cannot track this reference instantaneously due to the system mechanical inertia. Moreover, the position tracking is not affected by the load torque change at time $t = 1 \text{ s}$, because when the sliding surface is reached (sliding mode) the system becomes insensitive to the boundary external disturbances. In this figure a small overshoot can be observed, this overshoot can be eliminated reducing the controller gains; however, in this case the system response will be slower and then time employed to reach the reference position value will be higher.

The second graph shows the rotor position error and the third graph shows an enlarged scale of the rotor position error. This graph shows that after a small time the system tracks the reference with a zero error.

The fourth graph shows rotor speed and the fifth graph shows the motor torque and the load torque, as it can be seen in this graph, the motor torque steps from zero to 20 Nm at time 1 s because the load torque has been increased to 20 Nm.

The sixth graph shows the stator current i_A , and the seventh graph shows the sliding variable S .

Figure 5 shows the real test of the proposed variable structure position control for the induction motor using the experimental platform. The first graph shows the reference and the real rotor position. Like in the previous case (simulation test), the rotor position tracks the reference position in spite of system uncertainties. In this figures, a little can be observed due to the sensors used to make the system real measurements. As before, the position tracking is not affected by the load torque change at time $t = 1$ s, and a small overshoot can be observed.

The second graph shows the rotor position error and the third graph shows an enlarged scale of the rotor position error. This figure presents a small position error but the value of this error is similar to the encoder resolution, and therefore this is the minimal error value that can be measured in this experimental platform. It should be noted that a very small position error is obtained in the presence of a load torque, which is a difficult task to achieve for an induction motor.

The fourth graph shows rotor speed and the fifth graph shows the motor torque and the load torque; as in the previous case, the motor torque steps from zero to 20 Nm at time 1 s because the load torque has been increased to 20 Nm.

The sixth graph shows the stator current i_A , and the seventh graph shows the sliding variable S .

This experimental results can be compared with the experimental results presented in the paper [15]. In this sense, the performance of our control scheme presents a better performance than the control scheme of [15]. The position accuracy and the speed of the response are similar in both cases but the response of our controller is more quick than the response of the controller proposed in [15]. In this point it should be noted that in the real text are using a bigger induction motor whose inertia constant ($J = 5.7 \cdot 10^{-2}$ Kgm²) is greater than the motor inertia constant used in [15] ($J = 3.5 \cdot 10^{-4}$ Kgm²), which implies a major difficulty in order to accelerate the induction motor, and therefore in order to obtain a good speed response.

Moreover, our proposed algorithm is more straightforward than the algorithm presented in [15] and therefore presents a less computational cost, that is similar to the computational cost of the PID controller. This would be an interesting advantage in order to implement the controller in a low cost DSP-processor.

5. Conclusion. In this paper an induction motor position regulation using a sliding mode control for a real-time applications has been presented. In the design a field oriented vector control theory is employed in order to simplify the system dynamic equations.

In order to overcome the flux sensors, a flux estimator is also proposed, because the flux sensors increase the cost and reduce the reliability. The flux estimation algorithm is based on a Luenberger observer and employs the measured stator voltages and currents in the stationary reference frame.

The flux observer and the controller do not present a high computational cost and therefore the proposed control scheme can be implemented easily in a real-time applications using a low cost DSP-processor.

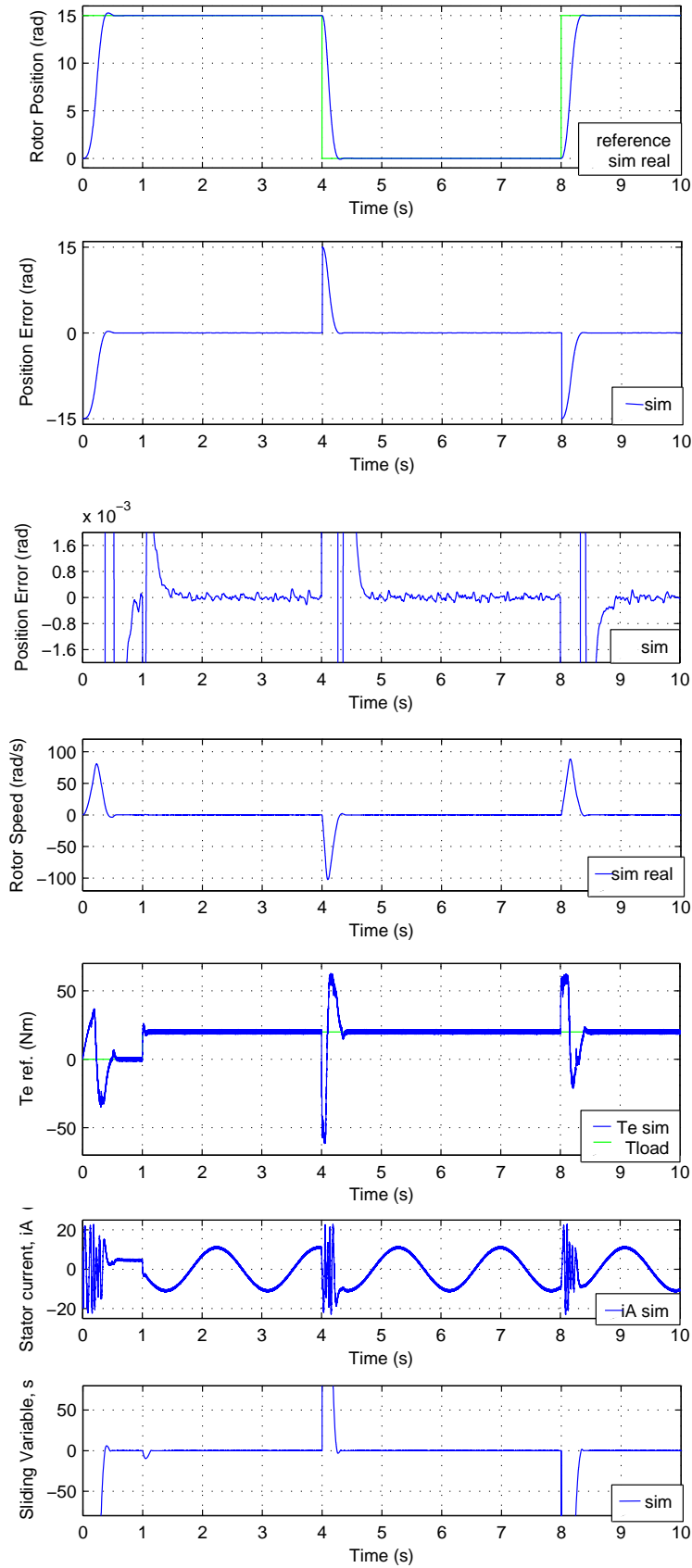


FIGURE 4. Square wave position reference simulation results

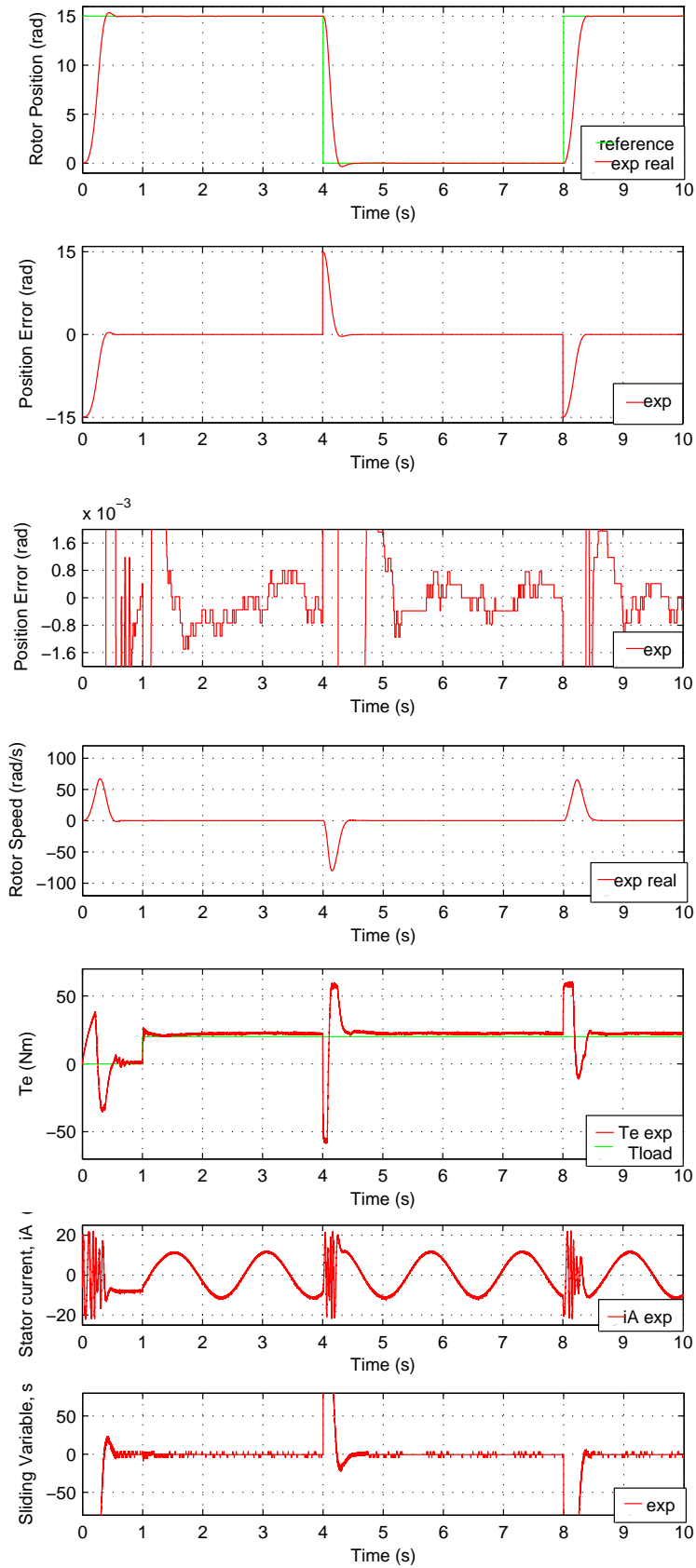


FIGURE 5. Square wave position reference experimental results

Due to the nature of the sliding mode control this control scheme is robust under uncertainties caused by parameter error or by changes in the load torque. The closed loop stability of the presented design has been proved through Lyapunov stability theory.

In order to demonstrate the performance of the proposed design over a commercial induction motor of 7.5 kW, a new experimental platform had to be designed and constructed to test the proposed robust controller in a real time application over a high power commercial induction motor.

Finally, by means of simulation and real examples, it has been confirmed that the proposed position control scheme presents a good performance in practice, and that the position tracking objective is achieved under parameter uncertainties and under load torque variations.

Acknowledgements. The authors are very grateful to the Basque Government by the support of this work through the project S-PE12UN015 and to the UPV/EHU by its support through the projects GUI10/01 and UFI11/07.

REFERENCES

- [1] P. Vas, *Vector Control of AC Machines*, Oxford Science Publications, Oxford, 1994.
- [2] W. Lehonhard, *Control of Electrical Drives*, Springer, Berlin, 1996.
- [3] R. Marino, P. Tomei and C. M. Verrelli, A nonlinear tracking control for sensorless induction motors, *Automatica*, vol.41, pp.1071-1077, 2005.
- [4] R. Yazdanpanah, J. Soltani and G. R. Arab Markadeh, Nonlinear torque and stator flux controller for induction motor drive based on adaptive input-output feedback linearization and sliding mode control, *Energy Conversion and Management*, vol.49, pp.541-550, 2008.
- [5] H. C. Cho, K. S. Lee and M. S. Fadali, Adaptive control of PMSM systems with chaotic nature using Lyapunov stability based feedback linearization, *International Journal of Innovative Computing, Information and Control*, vol.5, no.2, pp.479-488, 2009.
- [6] V. I. Utkin, Sliding mode control design principles and applications to electric drives, *IEEE Trans. Indus. Electro.*, vol.40, pp.26-36, 1993.
- [7] O. Barambones and P. Alkorta, A robust vector control for induction motor drives with an adaptive sliding-mode control law, *Journal of the Franklin Institute*, vol.348, pp.300-314, 2011.
- [8] C.-Y. Chen, Sliding mode controller design of induction motor based on space-vector pulse width modulation method, *International Journal of Innovative Computing, Information and Control*, vol.5, no.10(B), pp.3603-3614, 2009.
- [9] G. R. Lii, C. L. Chiang, C. T. Su and H. R. Hwung, An induction motor position controller optimally designed with fuzzy phase-plane control and genetic algorithms, *Electric Power Systems Research*, vol.68, pp.103-112, 2004.
- [10] D. Naso, F. Cupertino and B. Turchiano, Precise position control of tubular linear motors with neural networks and composite learning, *Control Engineering Practice*, vol.18, pp.515-522, 2010.
- [11] J. Yu, Y. Ma, B. Chen, H. Yu and S. Pan, Adaptive neural position tracking control for induction motors via backstepping, *International Journal of Innovative Computing, Information and Control*, vol.7, no.7(B), pp.4503-4516, 2011.
- [12] S. Kaitwanidvilai and A. Nath, Design and implementation of a high performance hard disk drive servo controller using GA based 2-DOF robust controller, *International Journal of Innovative Computing, Information and Control*, vol.8, no.2, pp.1025-1036, 2012.
- [13] A. Benchaib and C. Edwards, Nonlinear sliding mode control of an induction motor, *International Journal of Adaptive Control and Signal Processing*, vol.14, pp.201-221, 2000.
- [14] W. J. Wang and J. Y. Chen, Passivity-based sliding mode position control for induction motor drives, *IEEE Trans. on Energy conversion*, vol.20, pp.316-321, 2005.
- [15] B. Veselić, B. Peruničić-Dražnović and Č. Milosavljević, High-performance position control of induction motor using discrete-time sliding-mode control, *IEEE Trans. Ind. Electron.*, vol.55, no.11, pp.3809-3817, 2008.
- [16] M. Mena, O. Touhami, R. Ibtouen and M. Fadel, Sensorless direct vector control of an induction motor, *Control Engineering Practice*, vol.16, pp.67-77, 2008.

- [17] A. Takahashi and R. Oguro, Torque and speed estimation with parameter identification of line-start induction motor operated value, *International Journal of Innovative Computing, Information and Control*, vol.5, no.12(A), pp.4551-4559, 2009.
- [18] B. K. Bose, *Modern Power Electronics and AC Drives*, Prentice Hall, New Jersey, 2001.
- [19] O. Barambones, V. Etxebarria, Robust neural control for robotic manipulators, *Automatica*, vol.38, pp.235-242, 2002.